*Organometallics* 1990, *9*, 2709–2718

# Rotation of Coordinated Acetylide Ligands on the Triangular Surface of Trinuclear Heterometallic Clusters

Der-Kweng Hwang and Yun Chi*

*Department of Chemistry, National Tsing Hua University, Hsinchu 30043, Taiwan, Republic of China*

Shie-Ming Peng† and Gene-Hsiang Lee

*Department of Chemistry, National Taiwan University, Taipei 10764, Taiwan, Republic of China*

*Received February 26, 1990*

Convenient and widely applicable synthetic routes to the trinuclear heterometallic acetylide complexes $LMM'_2(CO)_8(C{\equiv}CR)$ have been developed. These routes involve the reaction of metal acetylides $LM(CO)_3(C{\equiv}CR)$ (L = Cp and Cp*; M = W and Mo; R = Ph, $C_5H_4F$, $C_5H_4OMe$, ${}^tBu$, and ${}^nPr$) with $Os_3(CO)_{10}(NCMe)_2$ and with $Ru_3(CO)_{12}$. For the $WOs_2$ derivatives prepared (**1**–**3**), the acetylide ligand adopts an asymmetric arrangement in which the acetylide C–C vector is coordinated to one of the W–Os bonds. For all the $WRu_2$ derivatives (**4**–**9**), the acetylide ligand adopts both the asymmetric (with its C–C bond orthogonal to one of the W–Ru bonds) and the symmetric arrangement (with its C–C bond orthogonal to the unique Ru–Ru bond) and undergoes rapid interconversion in solution. For the $MoRu_2$ derivatives (**10**, **11**), the acetylide favors the asymmetric form in both solution and the solid state; however, when the substituent R and the ligand L are replaced by a bulky *tert*-butyl group and Cp* ligand, respectively (**13**), the symmetric form becomes the dominant species. The dynamic $^{13}C$ NMR studies suggest that the acetylide ligand of the $WOs_2$ derivatives is static but, in the asymmetric $MoRu_2$ derivatives (**10**, **11**), the acetylide is fluxional and undergoes migration from one Mo–Ru edge to the other. The preference of the site selectivity for the acetylide ligand has also been studied by variation of the transition-metal atoms (M and M′), the accessory ligand (L), and the substituent (R). The structures of the complexes $CpWOs_2(CO)_8(C{\equiv}CPh)$ (**1**), $CpWRu_2(CO)_8(C{\equiv}CPh)$ (**4**), and $CpMoRu_2(CO)_8(C{\equiv}CPh)$ (**10**) have been determined by single-crystal X-ray diffraction studies. Crystal data for **1**: space group $P2_1/c$; $a$ = 8.332 (3) Å, $b$ = 14.543 (4) Å, $c$ = 17.819 (5) Å, $\beta$ = 94.46 (3)°, $Z$ = 4; final $R$ = 0.068, $R_w$ = 0.090, and GOF = 1.768. Crystal data for **4**: space group $P2_1/n$; $a$ = 12.476 (1) Å, $b$ = 13.216 (4) Å, $c$ = 13.395 (4) Å, $\beta$ = 97.99 (2)°, $Z$ = 4; final $R$ = 0.029, $R_w$ = 0.027, and GOF = 1.583. Crystal data for **10**: space group $P2_1/c$; $a$ = 12.770 (4) Å, $b$ = 8.188 (4) Å, $c$ = 21.313 (4) Å, $\beta$ = 91.26 (2)°, $Z$ = 4; final $R$ = 0.030, $R_w$ = 0.031, and GOF = 2.34.

## Introduction

The $C_2$ hydrocarbyl ligands occupy a key position in the development of dinuclear, trinuclear, and polynuclear organometallic chemistry. This position results partially from the belief that the chemistry of the $C_2$ hydrocarbyl ligands in the organometallic complexes is analogous to that of small hydrocarbon intermediates adsorbed on metal surfaces. Among the many interesting properties of the $C_2$ ligands is their mobility on the coordination sphere of the transition-metal complexes. Related studies on the $C_2$ hydrocarbyl moieties have attracted the attention of many theoretical and synthetic chemists.

Schilling and Hoffmann have reported the extended Hückel calculation of some hydrocarbons on the face of trinuclear homometallic transition-metal complexes.[1] For the trinuclear $C_2$ vinylidene complexes, Norton and Mislow have reported the disrotatory correlated rotation about the $Co_3(CO)_9$–C vector and C–CHR bond in $Co_3(CO)_9(CCHR)^+$ by variable-temperature $^{13}C$ NMR studies.[2] The motion of the vinylidene ligand in $H_3Os_3(CO)_9[C{=}\overline{CCH_2CH_2CH_2}]^+$ has also been described.[3] For the related $C_2$ alkyne complexes, the migration of the perpendicular alkyne ligand ($\mu_3$-$\eta^2$-$\perp$ mode) to the parallel position ($\mu_3$-$\eta^2$-$\|$ mode) upon electrochemical reduction has been documented for some trinuclear clusters,[4] whereas the alkyne ligand of the dinuclear heterometallic complexes $CpNiCo(CO)_3(RC{\equiv}CR')$ undergoes rotational motion about the Ni–Co bond vector.[5] In addition, both Stone and co-workers[6] and Shapley and co-workers[7] have described the "windscreen-wiper" type of motion for the coordinated alkyne ligand on a $W_2Os$ triangular face. Rosenberg and co-workers have reported the similar free rotation of the alkyne on the phosphine-substituted triosmium fragments.[8]

Recently, there has been growing research activity in the area of syntheses of acetylide cluster complexes.[9] However, to our knowledge, only a few papers have focused on the fluxional behavior of the acetylide ligand.[10] The reason is that, in the past, only the homometallic trinuclear acetylide complexes have been prepared. Therefore, it is difficult to distinguish whether the fluxional behavior of a target molecule is due to the rotation of acetylide or to

---

† To whom inquiries concerning the X-ray crystallographic work should be addressed.

[1] Schilling, B. E. R.; Hoffmann, R. *J. Am. Chem. Soc.* **1979**, *101*, 4687.

[2] Edidan, R. D.; Norton, J. R.; Mislow, K. *Organometallics* **1982**, *1*, 561.

[3] Koridze, A. A.; Kizas, O. A.; Kolobova, N. E.; Petrovskii, P. V.; Fedin, E. I. *J. Organomet. Chem.* **1984**, *265*, C33; **1984**, *272*, C31.

[4] Osella, D.; Goberto, R.; Montangero, P.; Zanello, P.; Cinquantini, A. *Organometallics* **1986**, *5*, 1247.

[5] Jaouen, G.; Marinetti, A.; Saillard, J.-Y.; Sayer, B. G.; McGlinchey, M. J. *Organometallics* **1982**, *1*, 225.

[6] Busetto, L.; Green, M.; Hesser, B.; Howard, J. A. K.; Jeffery, J. C.; Stone, F. G. A. *J. Chem. Soc., Dalton Trans.* **1983**, 519.

[7] Shapley, J. R.; Park, J. T.; Churchill, M. R.; Bueno, C.; Wasserman, H. J. *J. Am. Chem. Soc.* **1981**, *103*, 7385.

[8] Rosenberg, E.; Bracker-Novak, J.; Gellert, R. W.; Aime, S.; Gobetto, R.; Osella, D. *J. Organomet. Chem.* **1989**, *365*, 163.

[9] (a) Carty, A. J. *Pure Appl. Chem.* **1982**, *54*, 113. (b) Aime, S.; Osella, D.; Deeming, A. J.; Lanfredi, A. M. M.; Tiripicchio, A. *J. Organomet. Chem.* **1983**, *244*, C47. (c) Dawoodi, Z.; Mays, M. J.; Henrick, K. *J. Chem. Soc., Dalton Trans.* **1984**, 1769. (d) Deeming, A. J.; Donovan-Mtunzi, S.; Hardcastle, K. *J. Chem. Soc., Dalton Trans.* **1986**, 543. (e) Boyar, E.; Deeming, A. J.; Kabir, S. E. *J. Chem. Soc., Chem. Commun.* **1986**, 577. (f) Nucciarone, D.; MacLaughlin, S. A.; Taylor, N. J.; Carty, A. J. *Organometallics* **1988**, *7*, 106. (g) Galindo, A.; Mathieu, R.; Caminade, A.-M.; Majoral, J.-P. *Organometallics* **1988**, *7*, 2198. (h) Chi, Y.; Hwang, D.-K.; Chen, S.-F.; Liu, L.-K. *J. Chem. Soc., Chem. Commun.* **1989**, 1540. (i) Farrugia, L. J. *Organometallics* **1990**, *9*, 105.

[10] (a) Jangala, C.; Rosenberg, E.; Skinner, D.; Aime, S.; Milone, L.; Sappa, E. *Inorg. Chem.* **1980**, *19*, 1571. (b) Predieri, G.; Tiripicchio, A.; Vignali, C.; Sappa, E. *J. Organomet. Chem.* **1988**, *342*, C33.

0276-7333/90/2309-2709$02.50/0

the mobility of another accessory ligand, such as intermetallic CO scrambling.[11] In this paper, we report the preparation and crystal structure of a series of trinuclear $WOs_2$, $WRu_2$, and $MoRu_2$ acetylide complexes. Variable-temperature $^1H$ and $^{13}C$ NMR studies indicate that the acetylide ligand in some complexes undergoes rotation on the face of the heterometallic triangle. Furthermore, a systematic analysis of the preference of site selectivity and fluxional behavior of the acetylide ligand has been achieved by varying the transition-metal atom, the accessory ligand, and the substituent of the acetylide ligand. A portion of these results has appeared in a preliminary report.[12]

## Experimental Procedure

**General Information.** Infrared spectra were recorded on a Perkin-Elmer 580 spectrometer or on a Bomen M-100 FT-IR spectrometer. $^1H$ and $^{13}C$ NMR spectra were recorded with Bruker AM-400 (400.13 MHz) or Varian Gemini-300 (300 MHz) instruments. Mass spectra were obtained on a JEOL-HX110 instrument operating in electron impact or fast atom bombardment modes. All reactions were performed under a nitrogen atmosphere with use of deoxygenated solvents dried by an appropriate reagent. The progress of reactions was monitored by analytical thin-layer chromatography (5735 Kieselgel 60 $F_{254}$, E. Merck), and the products were separated on preparative thin-layer chromatographic plates (Kieselgel 60 $F_{254}$, E. Merck). Elemental analyses were performed by the staff of the NSC Regional Instrument Center at National Cheng Kung University, Tainan, Taiwan.

**Materials.** Metal carbonyl complexes and pentamethylcyclopentadiene were purchased from Strem Chemicals, Inc. Carbon monoxide enriched with 99% $^{13}C$ was purchased from Cambridge Isotope Laboratories. Phenylacetylene, 1-hexyne, and 1-pentyne were supplied by Aldrich Chemical Co., Inc. (4-fluorophenyl)acetylene and (4-methoxy)phenylacetylene was prepared from 4-fluoroacetophenone and 4-vinylanisole, respectively, according to the published procedures.[13,14] $CpW(CO)_3H$ was prepared by protonation of the sodium salt of the $CpW(CO)_3^-$ anion with acetic acid at ambient temperature, whereas $Cp^*W(CO)_3H$ was prepared by the reaction of pentamethylcyclopentadiene with $W(CO)_3(NCEt)_3$ in toluene at 100 °C.[15] On the other hand, the molybdenum hydride complexes $Cp^*Mo(CO)_3H$ and $CpMo(CO)_3H$ were prepared from the reaction of (*p*-xylene)$Mo(CO)_3$ with pentamethylcyclopentadiene and cyclopentadiene monomer, respectively.[16] Metal carbonyl chloride complexes $LM(CO)_3Cl$ were generated from the reactions of the respective hydrides with $CCl_4$ under nitrogen.[17] The metal acetylides $LM(CO)_3C{\equiv}CR$ and the triosmium acetonitrile complex $Os_3(CO)_{10}(CH_3CN)_2$ were prepared according to literature procedures.[18,19] $^{13}CO$-enriched acetylide complexes were prepared by equilibrating the acetylide complexes in a seal tube (25 mL) equipped with a Rotaflo stopcock under approximately 1 atm of 99% $^{13}CO$ at 100 °C in toluene overnight.

**Preparation of $CpWOs_2(CO)_8(C{\equiv}CPh)$.** As all the reactions of the metal acetylides $LM(CO)_3C{\equiv}CR$ with $Os_3(CO)_{12}$ were performed under similar conditions, the experimental details of only one reaction are reported here.

In a 100-mL round-bottom reaction flask, $Os_3(CO)_{12}$ (456 mg, 0.503 mmol) was treated with sublimed $Me_3NO$ (91 mg, 1.04 mmol) in a mixture of dichloromethane (50 mL) and acetonitrile (20 mL) at ambient temperature for 60 min. After evaporation of the solvent in vacuo, the acetylide complex $CpW(CO)_3C{\equiv}CPh$ (240 mg, 0.553 mmol) was added, and the reaction mixture was then dissolved in a toluene solution (30 mL) and brought to reflux for 30 min. Finally the solvent was evaporated, and the residue was separated by thin-layer chromatography (silica gel, dichloromethane:hexane = 1:1), giving 90 mg of $CpWOs_3(CO)_{11}(C{\equiv}CPh)$ as a red crystalline solid (0.073 mmol, 15%) and 35 mg of $CpWOs_2(CO)_8(C{\equiv}CPh)$ (**1a**) as a yellow crystalline solid (0.003 mmol, 8%). Crystals of **1a** suitable for an X-ray diffraction study were obtained from a layered solution of dichloromethane–methanol at room temperature. Spectroscopic data for complex **1a**: MS (FAB, $^{192}Os$, $^{184}W$) *m/z* 956 ($M^+$); IR ($C_6H_{12}$) $\nu$(CO) 2077 (s), 2043 (vs), 2005 (vs), 1995 (s), 1965 (s), 1924 (m) $cm^{-1}$; $^1H$ NMR ($CD_2Cl_2$, 294 K) $\delta$ 7.68 (d, 2 H), 7.37 (t, 2 H), 7.20 (t, 1 H), 5.29 (s, 5 H); $^{13}C$ NMR ($CD_2Cl_2$, 294 K) $\delta$ 208.3 ($J_{W-C}$ = 165 Hz, W—CO), 204.1 ($J_{W-C}$ = 157 Hz, W—CO), 179.4 (Os—CO), 137.5 (*C*CPh), 73.8 ($J_{W-C}$ = 16 Hz, C*C*Ph). Anal. Calcd for $C_{21}H_{10}O_8WOs_2$: C, 26.42; H, 1.06. Found: C, 26.40; H, 1.10.

**Carbonylation of $CpWOs_3(CO)_{11}(C{\equiv}CPh)$.** Toluene (40 mL) and the red tetrametallic acetylide complex $CpWOs_3(CO)_{11}(C{\equiv}CPh)$ (58 mg, 0.047 mmol) were combined in a 200-mL pressure bottle. A partial vacuum was drawn over the toluene solution; then the bottle was charged with carbon monoxide to a pressure of 30 psi. The bottle was then placed in a preheated oil bath, and the solution was stirred at 120 °C for 6 h. After the solvent was evaporated, the residue was separated by thin-layer chromatography (silica gel, dichloromethane:hexane = 1:1), giving 38 mg of $CpWOs_2(CO)_8(C{\equiv}CPh)$ (0.040 mmol, 85%) in addition to a trace amount of $Os_3(CO)_{12}$ (not determined).

**Preparation of $Cp^*WOs_2(CO)_8(C{\equiv}CPh)$.** The title complex (yield 2%) was prepared under conditions similar to those for complex **1a**, in addition to 10% of the red tetrametallic acetylide complex $Cp^*WOs_3(CO)_{11}(C{\equiv}CPh)$. Spectral data for complex **2a**: MS (FAB, $^{192}Os$, $^{184}W$) *m/z* 1026 ($M^+$); IR ($C_6H_{12}$) $\nu$(CO) 2076 (s), 2041 (vs), 2004 (vs), 1991 (s), 1963 (m), 1905 (w) $cm^{-1}$; $^1H$ NMR ($CDCl_3$, 294 K) $\delta$ 7.62 (d, 2 H), 7.31 (t, 2 H), 7.20 (t, 1 H), 1.93 (s, 15 H). Anal. Calcd for $C_{26}H_{20}O_8WOs_2$: C, 30.48; H, 1.97. Found: C, 30.38; H, 1.99.

**Preparation of $CpWOs_2(CO)_8(C{\equiv}C^nBu)$.** The title complex (yield 11%) was prepared under conditions similar to those for complex **1a**, in addition to 19% of the red tetranuclear acetylide complex $CpWOs_3(CO)_{11}(C{\equiv}C^nBu)$. Spectroscopic data for complex **3a**: MS (FAB, $^{192}Os$, $^{184}W$) *m/z* 936 ($M^+$); IR ($C_6H_{12}$) $\nu$(CO) 2075 (s), 2040 (vs), 2003 (vs), 1991 (s), 1975 (vw), 1961 (m), 1924 (w) $cm^{-1}$; $^1H$ NMR ($CDCl_3$, 294 K) $\delta$ 5.33 (s, 5 H), 3.04 (m, 2 H), 1.73 (m, 1 H), 1.61 (m, 1 H), 1.39 (m, 2 H), 0.93 (t, 3 H). Anal. Calcd for $C_{19}H_{14}O_8WOs_2$: C, 24.42; H, 1.51. Found: C, 24.33; H, 1.48.

**Preparation of $CpWRu_2(CO)_8(C{\equiv}CPh)$.** In a 50-mL round-bottom reaction flask, the metal acetylide $CpW(CO)_3C{\equiv}CPh$ (37 mg, 0.039 mmol) and $Ru_3(CO)_{12}$ (37 mg, 0.039 mmol) in toluene (35 mL) were heated to reflux for 30 min. After evaporation of the solvent in vacuo, the residue was separated by thin-layer chromatography (silica gel, hexane:dichloromethane = 1:1) and recrystallization, giving 20 mg of $CpWRu_2(CO)_8(C{\equiv}CPh)$ (**4**) as an orange crystalline material (0.018 mmol, 46%). Crystals of **4** suitable for X-ray structural determination were obtained by recrystallization from a layered solution of dichloromethane–methanol. Spectroscopic data for complex **4**: MS (FAB, $^{102}Ru$, $^{184}W$) *m/z* 778 ($M^+$); IR ($C_6H_{12}$) $\nu$(CO) 2076 (s), 2069 (m), 2044 (vs), 2033 (vs), 2010 (vs), 2003 (m), 1994 (m), 1975 (m), 1966 (w), 1952 (vw), 1930 (vw), 1918 (vw) $cm^{-1}$; $^1H$ NMR ($CDCl_3$, 294 K) $\delta$ 7.64–7.24 (m, Ph), 5.56 (s, Cp, **4b**), 5.25 (s, Cp, **4a**); $^{13}C$ NMR (THF-$d_8$, 294 K) $\delta$ 210.8 ($J_{W-C}$ = 160 Hz, W—CO, **4a**), 210.7 ($J_{W-C}$ = 165 Hz, W—CO, **4a**), 207.6 ($J_{W-C}$ = 169 Hz, W—CO, **4b**), 197.0 (Ru—CO, **4b**), 196.6 (Ru—CO, **4a**), 168.9 ($J_{W-C}$ = 139 Hz, *C*CPh, **4b**), 168.6 (*C*CPh, **4a**), 98.3 ($J_{W-C}$ = 22 Hz, C*C*Ph, **4b**), 85.6 ($J_{W-C}$ = 21 Hz, C*C*Ph, **4a**). Anal. Calcd for $C_{21}H_{10}O_8WRu_2$: C, 32.49; H, 1.30. Found: C, 32.37; H, 1.35.

**Preparation of $Cp^*WRu_2(CO)_8(C{\equiv}CPh)$.** The toluene solution of a mixture of $Ru_3(CO)_{12}$ (100 mg, 0.156 mmol) and

---

[11] Rosenberg, E.; Milone, L.; Aime, S. *Inorg. Chim. Acta* **1975**, *15*, 33.

[12] Chi, Y.; Liu, B.-J.; Lee, G.-H.; Peng, S.-H. *Polyhedron* **1989**, *8*, 2003.

[13] Lambert, J. B.; Larson, E. G.; Bosch, R. J.; TeVrucht, M. L. E. *J. Am. Chem. Soc.* **1985**, *107*, 5443.

[14] (a) Newman, M. S.; Dhawan, B.; Hashem, M. M.; Khanna, V. K.; Springer, J. M. *J. Org. Chem.* **1976**, *41*, 3925. (b) Vaughn, T. H.; Vogt, R. R.; Nieuwland, J. A. *J. Am. Chem. Soc.* **1934**, *56*, 2120.

[15] Kubas, G. L.; Wasserman, H. J.; Ryan, R. R. *Organometallics* **1985**, *4*, 2012. (b) Kubas, G. J. *Inorg. Chem.* **1983**, *22*, 692.

[16] Nolan, S. P.; Hoff, C. D. In *Organometallic Syntheses*; King, R. B., Eisch, J. J., Eds.; Elsevier: New York, 1989; Vol. 4, p 58.

[17] Piper, T. S.; Wilkinson, G. *J. Inorg. Nucl. Chem.* **1956**, *3*, 104.

[18] Bruce, M. I.; Humphrey, M. G.; Matisons, J. G.; Roy, S. K.; Swincer, A. G. *Aust. J. Chem.* **1984**, *37*, 1955.

[19] Johnson, B. F. G.; Lewis, J.; David, A. P. *J. Chem. Soc., Dalton Trans.* **1981**, 407.

Cp*W(CO)$_3$C$\equiv$CPh (90 mg, 0.178 mmol) was heated at reflux for 30 min. After TLC separation and recyrstallization, the acetylide complex Cp*WRu$_2$(CO)$_8$(C$\equiv$CPh) (**5**; 86 mg, 0.10 mmol) was obtained in 57% yield. Spectroscopic data for complex **5**: MS (FAB, $^{102}$Ru, $^{184}$W) *m/z* 848 (M$^+$); IR (C$_6$H$_{12}$) ν(CO) 2071 (m), 2064 (vs), 2038 (s), 2024 (vs), 2005 (s), 2001 (vs), 1986 (m), 1970 (w), 1965 (w), 1955 (w), 1936 (vw), 1913 (vw) cm$^{-1}$; $^1$H NMR (CD$_2$Cl$_2$, 273 K) δ 7.65–7.27 (m, Ph), 2.30 (s, Me, **5b**), 1.93 (s, Me, **5a**); $^{13}$C NMR (THF-*d*$_8$, 226 K) δ 218.5 (W—CO, **5a**), 217.3 (W—CO, **5a**), 214.5 ($J_{W-C}$ = 169 Hz, W—CO, **5b**), 175.3 (*C*CPh, **5b**), 173.0 ($J_{W-C}$ = 141 Hz, *C*CPh, **5a**), 100.1 ($J_{W-C}$ = 23 Hz, C*C*Ph, **5b**), 90.2 (C*C*Ph, **5a**). Anal. Calcd for C$_{26}$H$_{20}$O$_8$WRu$_2$: C, 36.89; H, 2.38. Found: C, 36.86; H, 2.42.

**Preparation of CpWRu$_2$(CO)$_8$(C$\equiv$CC$_6$H$_4$F).** The toluene solution of a mixture of Ru$_3$(CO)$_{12}$ (75 mg, 0.117 mmol) and CpW(CO)$_3$C$\equiv$CC$_6$H$_4$F (80 mg, 0.177 mmol) was heated at reflux for 30 min. After TLC separation and recrystallization, the acetylide complex CpWRu$_2$(CO)$_8$(C$\equiv$CC$_6$H$_4$F) (**6**; 73 mg, 0.091 mmol) was obtained in 52% yield. Spectroscopic data for complex **6**: MS (FAB, $^{102}$Ru, $^{184}$W) *m/z* 796 (M$^+$); IR (C$_6$H$_{12}$) ν(CO) 2075 (s), 2069 (s), 2042 (vs), 2032 (vs), 2009 (vs, br), 1994 (m), 1979 (vw), 1972 (m), 1963 (w), 1949 (vw), 1928 (vw), 1914 (vw) cm$^{-1}$; $^1$H NMR (CDCl$_3$, 294 K) δ 7.63 (m, 1 H), 7.52 (m, 1 H), 7.02 (m, 2 H), 5.57 (s, Cp, **6b**), 5.25 (s, Cp, **6a**); $^{13}$C NMR (CDCl$_3$, 294 K) δ 211.3 (W—CO, **6a**), 210.8 (W—CO, **6a**), 207.7 ($J_{W-C}$ = 169 Hz, W—CO, **6b**), 196.9 (Ru—CO, **6b**), 196.5 (Ru—CO, **6a**), 88.4 (Cp, **6a**), 86.2 (Cp, **6b**). Anal. Calcd for C$_{21}$H$_9$FO$_8$WRu$_2$: C, 31.76; H, 1.14. Found: C, 31.68; H, 1.13.

**Preparation of CpWRu$_2$(CO)$_8$(C$\equiv$CC$_6$H$_4$OMe).** The toluene solution of a mixture of Ru$_3$(CO)$_{12}$ (165 mg, 0.248 mmol) and CpW(CO)$_3$C$\equiv$CC$_6$H$_4$OMe (180 mg, 0.388 mmol) was heated at reflux for 30 min. After TLC separation and recrystallization, the acetylide complex CpWRu$_2$(CO)$_8$(C$\equiv$CC$_6$H$_4$OMe) (**7**; 162 mg, 0.200 mmol) was obtained in 52% yield. Spectroscopic data for complex **7**: MS (FAB, $^{102}$Ru, $^{184}$W) *m/z* 808 (M$^+$); IR (C$_6$H$_{12}$) ν(CO) 2077 (s), 2070 (s), 2043 (vs), 2033 (vs), 2011 (vs, br), 1991 (m), 1972 (m), 1964 (w), 1948 (vw), 1928 (vw), 1913 (vw) cm$^{-1}$; $^1$H NMR (toluene-*d*$_8$, 244 K) δ 7.95 (d, 1.18 H, **7b**), 7.84 (d, 0.82 H, **7a**), 6.90 (d, 0.82 H, **7a**), 6.78 (d, 1.18 H, **7b**), 4.63 (s, 2.95 H, Cp, **7b**), 4.45 (s, 2.05 H, Cp, **7a**), 3.52 (s, 2.05 H, OMe, **7a**), 3.41 (s, 2.95 H, OMe, **7b**); $^{13}$C NMR (CDCl$_3$, 244 K) δ 211.3 (W—CO, **7a**), 210.8 (W—CO, **7a**), 207.7 ($J_{W-C}$ = 178 Hz, W—CO, **7b**), 196.7 (br, Ru—CO), 166.1 (*C*CAr, **7b**), 165.1 (*C*CAr, **7a**), 98.6 (C*C*Ar, **7b**), 84.6 (C*C*Ar, **7a**), 88.4 (Cp, **7a**), 86.0 (Cp, **7b**). Anal. Calcd for C$_{22}$H$_{12}$O$_9$WRu$_2$: C, 32.77; H, 1.50. Found: C, 32.72; H, 1.47.

**Preparation of CpWRu$_2$(CO)$_8$(C$\equiv$C$^t$Bu).** The toluene solution of a mixture of Ru$_3$(CO)$_{12}$ (189 mg, 0.296 mmol) and CpW(CO)$_3$C$\equiv$C$^t$Bu (184 mg, 0.443 mmol) was heated at reflux for 40 min. After TLC separation and recrystallization, the acetylide complex CpWRu$_2$(CO)$_8$(C$\equiv$C$^t$Bu) (**8**); 223 mg, 0.294 mmol) was obtained in 66% yield. Selected spectroscopic data for complex **8**: MS (FAB, $^{102}$Ru, $^{184}$W) *m/z* 758 (M$^+$); IR (C$_6$H$_{12}$) ν(CO) 2074 (w), 2068 (vs), 2039 (w), 2031 (vs), 2005 (vs), 1991 (s), 1981 (w), 1971 (w), 1961 (m), 1928 (w, br) cm$^{-1}$; $^1$H NMR (CDCl$_3$, 294 K) δ 5.47 (s, 4.8 H, **8b**), 5.38 (s, 0.2 H, **8a**), 1.42 (s, 0.36 H, **8a**), 1.35 (s, 8.64 H, **8b**). $^{13}$C NMR (CD$_2$Cl$_2$, 294 K) δ 211.8 (W—CO, **8a**), 209.9 (W—CO, **8a**), 208.0 ($J_{W-C}$ = 172 Hz, W—CO, **8b**), 197.6 (Ru—CO, **8b**), 196.9 (Ru—CO, **8a**), 87.1 (Cp, **8a**), 86.1 (Cp, **8b**). Anal. Calcd for C$_{19}$H$_{14}$O$_8$WRu$_2$: C, 30.17; H, 1.87. Found: C, 30.08; H, 1.86.

**Preparation of CpWRu$_2$(CO)$_8$(C$\equiv$C$^n$Pr).** The toluene solution of a mixture of Ru$_3$(CO)$_{12}$ (223 mg, 0.349 mmol) and CpW(CO)$_3$C$\equiv$C$^n$Pr (210 mg, 0.524 mmol) was heated at reflux for 30 min. After TLC separation and recrystallization, the acetylide complex CpWRu$_2$(CO)$_8$(C$\equiv$C$^n$Pr) (**9**; 221 mg, 0.298 mmol) was isolated in 57% yield. Selected spectroscopic data for complex **9**: MS (FAB, $^{102}$Ru, $^{184}$W) *m/z* 744 (M$^+$); IR (C$_6$H$_{12}$) ν(CO) 2074 (w), 2068 (s), 2040 (m), 2030 (vs), 2005 (vs), 1998 (m), 1991 (s), 1980 (vw), 1970 (w), 1960 (m), 1924 (vw, br) cm$^{-1}$; $^1$H NMR (CDCl$_3$, 294 K) δ 5.49 (s, 4 H, **9b**), 5.31 (s, 1 H, **9a**), 2.93 (t, 0.4 H, **9a**), 2.84 (t, 1.6 H, **9b**), 1.81 (m, 0.4 H, **9a**), 1.68 (m, 1.6 H, **9b**), 1.00 (t, 0.6 H, **9a**), 0.98 (t, 2.4 H, **9b**); $^{13}$C NMR (CD$_2$Cl$_2$, 294 K) δ 211.6 ($J_{W-C}$ = 163 Hz, W—CO, **9a**), 210.1 ($J_{W-C}$ = 166 Hz, W—CO, **9a**), 208.2 ($J_{W-C}$ = 170 Hz, W—CO, **9b**), 197.2 (Ru—CO, **9b**), 196.8 (Ru—CO, **9a**), 163.1 (*C*C$^n$Pr, **9a**), 161.9 ($J_{W-C}$ = 139 Hz, *C*C$^n$Pr, **9b**), 97.9 ($J_{W-C}$ = 22 Hz, C*C*$^n$Pr, **9b**), 87.7 (Cp, **9a**), 87.0 (C*C*$^n$Pr, **9a**), 86.2 (Cp, **9b**). Anal. Calcd for C$_{18}$H$_{12}$O$_8$WRu$_2$: C, 29.11; H, 1.62. Found: C, 29.10; H, 1.59.

**Preparation of CpMoRu$_2$(CO)$_8$(C$\equiv$CPh).** The toluene solution of a mixture of Ru$_3$(CO)$_{12}$ (357 mg, 0.559 mmol) and CpMo(CO)$_3$C$\equiv$CPh (290 mg, 0.838 mmol) was heated at reflux for 40 min. After TLC separation and recrystallization, the acetylide complex CpMoRu$_2$(CO)$_8$(C$\equiv$CPh) (**10a**; 244 mg, 0.353 mmol) was isolated in 42% yield. Selected spectroscopic data for complex **10a**: MS (FAB, $^{102}$Ru, $^{98}$Mo) *m/z* 692 (M$^+$); IR (C$_6$H$_{12}$) ν(CO) 2078 (vs), 2045 (vs), 2012 (vs), 2005 (s), 1978 (m), 1948 (w), 1920 (vw, br) cm$^{-1}$; $^1$H NMR (CDCl$_3$, 294 K) δ 7.64 (d, 2 H), 7.35 (t, 2 H), 7.26 (t, 1 H), 5.14 (s, 5 H); $^{13}$C NMR (CDCl$_3$, 294 K) δ 226.8 (Mo—CO, 1 C), 225.3 (Mo—CO, 1 C), 197.9 (Ru—CO, 3 C), 196.4 (Ru—CO, 3C, broad), 91.0 (Cp, 5 C). Anal. Calcd for C$_{21}$H$_{10}$O$_8$MoRu$_2$: C, 36.64; H, 1.46. Found: C, 36.51; H, 1.46.

**Preparation of Cp*MoRu$_2$(CO)$_8$(C$\equiv$CPh).** The toluene solution of a mixture of Ru$_3$(CO)$_{12}$ (300 mg, 0.469 mmol) and Cp*Mo(CO)$_3$C$\equiv$CPh (293 mg, 0.704 mmol) was heated at reflux for 30 min. After TLC separation and recrystallization, the acetylide complex Cp*MoRu$_2$(CO)$_8$(C$\equiv$CPh) (**11a**; 304 mg, 0.399 mmol) was isolated in 57% yield. Selected spectroscopic data for complex **11a**: MS (FAB, $^{102}$Ru, $^{98}$Mo) *m/z* 762 (M$^+$); IR (C$_6$H$_{12}$) ν(CO) 2072 (vs), 2040 (vs), 2007 (vs), 1999 (s), 1971 (s), 1972 (w, br), 1885 (w, br) cm$^{-1}$; $^1$H NMR (CDCl$_3$, 294 K) δ 7.59 (d, 2 H), 7.31 (t, 2 H), 7.22 (t, 1 H), 1.76 (s, 15 H); $^{13}$C NMR (CDCl$_3$, 244 K) δ 230.0 (Mo—CO, 1 C), 229.4 (Mo—CO, 1 C), 201.4 (Ru—CO, 1 C), 197.6 (Ru—CO, 3C), 193.7 (Ru—CO, 1 C), 192.8 (Ru—CO, 1 C), 175.3 (*C*CPh), 94.5 (C*C*Ph), 103.1 (*C*$_5$Me$_5$). Anal. Calcd for C$_{26}$H$_{20}$O$_8$MoRu$_2$: C, 41.17; H, 2.66. Found: C, 41.13; H, 2.66.

**Preparation of CpMoRu$_2$(CO)$_8$(C$\equiv$C$^t$Bu).** The toluene solution of a mixture of Ru$_3$(CO)$_{12}$ (131 mg, 0.205 mmol) and CpMo(CO)$_3$C$\equiv$C$^t$Bu (104 mg, 0.319 mmol) was heated at reflux for 40 min. After TLC separation and recrystallization, the acetylide complex CpMoRu$_2$(CO)$_8$(C$\equiv$C$^t$Bu) (**12**; 80 mg, 0.119 mmol) was isolated in 37% yield. Selected spectroscopic data for complex **12**: MS (FAB, $^{102}$Ru, $^{98}$Mo) *m/z* 672 (M$^+$); IR (C$_6$H$_{12}$) ν(CO) 2076 (s), 2070 (w), 2041 (vs), 2032 (m), 2010 (vs), 1999 (s), 1974 (m), 1951 (vw), 1917 (vw) cm$^{-1}$; $^1$H NMR (CDCl$_3$, 244 K) δ 5.43 (s, 5 H, **12a**), 5.34 (s, **12b**), 1.38 (s, **12b**), 1.33 (s, 9 H, **12a**); $^{13}$C NMR (CD$_2$Cl$_2$, 205 K) δ 225.9 (Mo—CO, 1 C, **12a**), 225.5 (Mo—CO, 1 C, **12a**), 223.0 (Mo—CO, 2 C, **12b**), 204.0 (Ru—CO, 1 C, **12a**), 202.4 (Ru—CO, 1 C, **12a**), 200.1 (Ru—CO, 6 C, **12b**), 197.4 (Ru—CO, 1 C, **12a**), 196.4 (Ru—CO, 1 C, **12a**), 194.8 (Ru—CO, 1 C, **12a**), 194.3 (Ru—CO, 1 C, **12a**). Anal. Calcd for C$_{19}$H$_{14}$O$_8$MoRu$_2$: C, 34.14; H, 2.11. Found: C, 33.92; H, 2.04.

**Preparation of Cp*MoRu$_2$(CO)$_8$(C$\equiv$C$^t$Bu).** The toluene solution of a mixture of Ru$_3$(CO)$_{12}$ (43 mg, 0.067 mmol) and Cp*Mo(CO)$_3$C$\equiv$C$^t$Bu (40 mg, 0.101 mmol) was heated at reflux for 60 min. After TLC separation and recrystallization, the acetylide complex Cp*MoRu$_2$(CO)$_8$(C$\equiv$C$^t$Bu) (**13b**; 27 mg, 0.036 mmol) was isolated in 36% yield. Selected spectroscopic data for complex **13b**: MS (FAB, $^{102}$Ru, $^{98}$Mo) *m/z* 742 (M$^+$); IR (C$_6$H$_{12}$) ν(CO) 2062 (s), 2023 (vs), 1999 (vs), 1986 (s), 1963 (w), 1951 (w), 1912 (vw, br) cm$^{-1}$; $^1$H NMR (CDCl$_3$, 294 K) δ 2.08 (s, 15 H), 1.38 (s, 9 H); $^{13}$C NMR (CDCl$_3$, 294 K) δ 227.3 (Mo—CO), 199.1 (Ru—CO), 186.8 (*C*C$^t$Bu), 115.8 (C*C*$^t$Bu), 103.9 (*C*$_5$Me$_5$), 35.5 (*C*Me$_3$), 34.8 (5 Me), 11.6 (3 Me); $^{13}$C NMR (CD$_2$Cl$_2$, 200 K) δ 227.0 (Mo—CO, 2 C), 207.0 (Ru—CO, broad, 2 C), 200.6 (Ru—CO, broad, 2 C), 191.0 (Ru—CO, broad, 2 C). Anal. Calcd for C$_{24}$H$_{24}$O$_8$MoRu$_2$: C, 39.03; H, 3.28. Found: C, 38.99; H, 3.25.

**Preparation of CpMoRu$_2$(CO)$_8$(C$\equiv$CC$_6$H$_4$F).** The toluene solution of a mixture of Ru$_3$(CO)$_{12}$ (193 mg, 0.302 mmol) and CpMo(CO)$_3$C$\equiv$CC$_6$H$_4$F (165 mg, 0.453 mmol) was heated at reflux for 30 min. After TLC separation and recrystallization, the acetylide complex CpMoRu$_2$(CO)$_8$(C$\equiv$CC$_6$H$_4$F) (**14a**; 127 mg, 0.179 mmol) was isolated in 40% yield. Selected spectroscopic data for complex **14a**: MS (FAB, $^{102}$Ru, $^{98}$Mo) *m/z* 710 (M$^+$); IR (C$_6$H$_{12}$) ν(CO) 2077 (vs), 2044 (vs), 2011 (vs), 2004 (s), 1986 (vw), 1976 (s), 1948 (m), 1914 (w) cm$^{-1}$; $^1$H NMR (CDCl$_3$, 294 K) δ 7.62 (m, 2 H), 7.04 (m, 2 H), 5.15 (s, 5 H); $^{13}$C NMR (CDCl$_3$, 294 K) δ 226.7 (Mo—CO, 1 C), 225.1 (Mo—CO, 1 C), 197.8 (Ru—CO, 3 C), 196.4 (Ru—CO, broad, 3 C), 171.8 (*C*CAr), 91.6 (C*C*Ar), 90.8 (Cp, 5 C). Anal. Calcd for C$_{21}$H$_9$FO$_8$MoRu$_2$: C, 35.71; H, 1.28. Found: C, 35.63; H, 1.28.

**X-ray Crystallography.** Diffraction measurements were carried out on a Nonius CAD-4 fully automatic four-circle dif-

**Table I. Experimental Data for the X-ray Diffraction Studies of Complexes 1, 4, and 10**[a]

| compd | 1 | 4 | 10 |
|---|---|---|---|
| formula | $C_{21}H_{10}O_8Os_2W$ | $C_{21}H_{10}O_8Ru_2W$ | $C_{21}H_{10}O_8MoRu_2$ |
| mol wt | 1104.27 | 776.29 | 688.39 |
| cryst syst | monoclinic | monoclinic | monoclinic |
| space group | $P2_1/c$ | $P2_1/n$ | $P2_1/c$ |
| $a$, Å | 8.332 (3) | 12.476 (1) | 12.770 (4) |
| $b$, Å | 14.543 (4) | 13.216 (4) | 8.188 (4) |
| $c$, Å | 17.819 (5) | 13.395 (4) | 21.313 (4) |
| $\beta$, deg | 94.46 (3) | 97.99 (2) | 91.26 (2) |
| $V$, Å$^3$ | 2153 (1) | 2187 (1) | 2228 (1) |
| $Z$ | 4 | 4 | 4 |
| $D_c$, g/cm$^3$ | 2.945 | 2.358 | 2.052 |
| $F(000)$ | 1703.33 | 1447.68 | 1319.70 |
| temp, K | 297 | 297 | 297 |
| scan method | $\theta/2\theta$ scan mode | $\theta/2\theta$ scan mode | $\theta/2\theta$ scan mode |
| $2\theta$(max), deg | 49.8 | 49.8 | 49.8 |
| scan param | $0.65 + 0.35 \tan\theta$ | $0.65 + 0.35 \tan\theta$ | $0.65 + 0.35 \tan\theta$ |
| scan speed (variable), deg/min | 16.48/10–16.48/2 | 16.48/10–16.48/2 | 16.48/10–16.48/2 |
| $h,k,l$ ranges | −9 to 9, 0–17, 0–21 | −14 to 14, 0–15, 0–15 | −15 to 15, 0–9, 0–25 |
| cryst size, mm | 0.25 × 0.40 × 0.50 | 0.20 × 0.20 × 0.25 | 0.08 × 0.18 × 0.55 |
| abs cor | $\psi$ scan | $\psi$ scan | $\psi$ scan |
| $\mu$(Mo K$\alpha$), mm$^{-1}$ | 17.28 | 6.74 | 1.90 |
| transmissn factors: max, min | 0.998, 0.371 | 0.997, 0.796 | 1.000, 0.839 |
| variation of std rflns, % | <3 (every 3600 s) | <2 (every 7200 s) | <2 (every 7200 s) |
| no. of unique rflns | 3777 | 3840 | 3907 |
| no. of data with $I > 2\sigma(I)$ | 2980 | 2851 | 3089 |
| weighting scheme | unit weight | $1/\sigma^2$ (counting statistic) | $1/\sigma^2$ |
| no. of atoms and params refined | 42, 145 | 42, 290 | 42, 290 |
| max $\Delta/\sigma$ ratio | 0.043 | 0.467 | 2.484 |
| $R$; $R_w$[b] | 0.068; 0.090 | 0.029; 0.027 | 0.030; 0.031 |
| GOF[c] | 1.768 | 1.583 | 2.34 |
| max/min residual electron density, e/Å$^3$ | 2.30–1.35 | 0.80–0.58 | 0.42–0.65 |

[a] Features common to all determinations: $\lambda$(Mo K$\alpha$) = 0.709 30 Å; Nonium CAD-4 diffractometer. [b] $R = \sum|F_o - F_c|/\sum|F_o|$; $R_w = [\sum w|F_o - F_c|^2//\sum w|F_o|^2]^{1/2}$. [c] $\mathrm{GOF} = [\sum w|F_o - F_c|^2/(N_0 - N_v)]^{1/2}$ ($N_o$ = number of observations; $N_v$ = number of variables).

fractometer. In general, the space group and parameters of unit cell dimensions were determined and refined from 25 randomly selected reflections, with a $2\theta$ angle about 20°, obtained by using the CAD-4 automatic search, center, index, and least-squares routines. All data reduction and structural refinement were performed by using the NRCC-SDP-VAX software packages. The structures were solved by the heavy-atom method and refined by least-squares cycles. For complex **1**, the tungsten and the osmium metal atoms were refined anisotropically and the rest of the non-hydrogen atoms were refined isotropically. For complexes **4** and **10**, all non-hydrogen atoms were refined with anisotropic thermal parameters; the hydrogen atoms of the phenyl group and the cyclopentadienyl ligand were added at the idealized positions and included in the structure factor calculations. The data collection and refinement parameters for complexes **1**, **4**, and **10** are summarized in Table I. Atomic positional parameters for complex **1** are found in Table II, whereas some selected bond angles and lengths are given in Table V. The corresponding parameters for complex **4** are given in Tables III and VI and for complex **10** in Tables IV and VII, respectively.

## Results and Discussion

**Preparation of the WOs$_2$ Acetylide Complexes.** Treatment of $LW(CO)_3C{\equiv}CR$ (R = Ph, L = Cp, Cp*; R = $^n$Bu, L = Cp) with the lightly stabilized triosmium complex $Os_3(CO)_{10}(CH_3CN)_2$ in refluxing toluene (110 °C, 30 min) provided a pale yellow trinuclear heterometallic acetylide complex (**1**, L = Cp, R = Ph; **2**, L = Cp*, R = Ph; **3**, L = Cp, R = $^n$Bu) in low yield (2–11%), in addition to the red tetrametallic complex $LWOs_3(CO)_{11}(C{\equiv}CR)$ (10–19%).[20] Thermolysis of the tetrametallic acetylide complexes under a CO atmosphere induced cluster fragmentation and produced the trinuclear WOs$_2$ acetylide complexes in high yield (78–85%). The latter has been considered as an alternative, complementary method to generate large quantities of the WOs$_2$ acetylide complexes in our laboratory. Furthermore, other chemistry of these WOs$_3$ acetylide complexes, such as the reactions with disubstituted alkynes[21] and with mononuclear metal acetylide complexes,[22] has also been developed.

The structural information of these WOs$_2$ acetylide complexes was initially provided by a $^{13}$C NMR study. The $^{13}C\{^1H\}$ NMR spectrum of **1** showed two signals at $\delta$ 137.5 and 73.8, reminiscent of those reported for the two acetylide carbon nuclei ($\delta$ 172.9 and 112.7) in the WFe$_2$ analogue $CpWFe_2(CO)_8(C{\equiv}CTol)$.[23] The latter is a heterometallic cluster in which the acetylide ligand functions as a five-electron donor, $\sigma$-bonded to the tungsten atom while employing its two orthogonal alkyne $\pi$-bonds to bridge the unique Fe–Fe edge. However, since the color as well as the IR spectra of these osmium complexes in the region of CO absorption differs substantially from those of the WFe$_2$ derivatives, an X-ray diffraction study was carried out on complex **1** to determine the location of the acetylide ligand in the WOs$_2$ derivatives.

**Description of the Structure of $CpWOs_2(CO)_8(C{\equiv}CPh)$ (1).** As indicated in Figure 1, this molecule has a triangular WOs$_2$ core structure with distances W–Os(1) = 2.830 (2) Å, W–Os(2) = 2.916 (2) Å, and Os(1)–Os(2) = 2.814 (2) Å, in which the tungsten atom is associated with a Cp ring and two CO ligands, while each of the osmium atoms is linked to three, mutually orthogonal, terminal CO ligands. The acetylide moiety is coordinated to the WOs$_2$ triangular face with its $\alpha$-carbon bound to all three metal atoms with bond distances W–C(15) = 2.20 (3) Å, Os-

---

(20) Chi, Y.; Lee, G.-H.; Peng, S.-H.; Wu, C.-H. *Organometallics* **1989**, *8*, 1574.

(21) Wu, C.-H.; Chi, Y.; Peng, S.-H.; Lee, G.-H. *Organometallics*, in press.

(22) Wu, C.-H.; Chi, Y.; Peng, S.-H.; Lee, G.-H. *J. Chem. Soc., Dalton Trans.*, in press.

(23) Green, M.; Marsden, K.; Salter, I. D.; Stone, F. G. A.; Woodward, P. *J. Chem. Soc., Chem. Commun.* **1983**, 446.

**Table II. Atomic Coordinates and Equivalent Isotropic Displacement Coefficients for $CpWOs_2(CO)_8(C{\equiv}CPh)$ (1)**

| | $x$ | $y$ | $z$ | $B_{iso}$,$^a$ Å$^2$ |
|---|---|---|---|---|
| Os(1) | 0.48889 (14) | 0.81811 (8) | 0.16703 (6) | 1.35 (5) |
| Os(2) | 0.26829 (15) | 0.96203 (8) | 0.13507 (6) | 1.55 (5) |
| W | 0.22595 (14) | 0.83355 (8) | 0.25760 (6) | 1.24 (4) |
| C(1) | 0.416 (4) | 0.7582 (21) | 0.0798 (17) | 1.6 (5) |
| C(2) | 0.619 (4) | 0.7191 (21) | 0.2004 (17) | 1.6 (5) |
| C(3) | 0.654 (4) | 0.8829 (23) | 0.1258 (19) | 2.2 (6) |
| C(4) | 0.105 (5) | 1.043 (3) | 0.1568 (21) | 2.9 7) |
| C(5) | 0.154 (4) | 0.9141 (24) | 0.0470 (19) | 2.3 (6) |
| C(6) | 0.393 (4) | 1.046 (3) | 0.0810 (20) | 2.6 (6) |
| C(7) | 0.314 (4) | 0.7106 (21) | 0.2740 (17) | 1.8 (5) |
| C(8) | 0.113 (4) | 0.7723 (23) | 0.1687 (19) | 2.3 (6) |
| C(9) | 0.118 (4) | 0.8041 (24) | 0.3731 (20) | 2.4 (6) |
| C(10) | 0.188 (4) | 0.8884 (24) | 0.3791 (19) | 2.4 (6) |
| C(11) | 0.118 (5) | 0.947 (3) | 0.3249 (22) | 3.2 (7) |
| C(12) | −0.012 (5) | 0.900 (3) | 0.2848 (21) | 2.9 (7) |
| C(13) | −0.014 (4) | 0.8120 (24) | 0.3133 (20) | 2.5 (6) |
| C(14) | 0.491 (5) | 0.891 (3) | 0.2734 (21) | 3.0 (7) |
| C(15) | 0.405 (3) | 0.9351 (19) | 0.2272 (15) | 1.0 (4) |
| C(16) | 0.589 (4) | 0.8897 (22) | 0.3458 (18) | 2.0 (5) |
| C(17) | 0.648 (4) | 0.978 (3) | 0.3692 (21) | 2.8 (7) |
| C(18) | 0.753 (5) | 0.985 (3) | 0.434 (3) | 4.1 (9) |
| C(19) | 0.793 (6) | 0.908 (4) | 0.475 (3) | 4.9 (10) |
| C(20) | 0.736 (5) | 0.826 (3) | 0.4554 (23) | 3.6 (8) |
| C(21) | 0.630 (5) | 0.813 (3) | 0.3874 (21) | 3.0 (7) |
| O(1) | 0.360 (3) | 0.7252 (20) | 0.0233 (16) | 3.9 (6) |
| O(2) | 0.702 (4) | 0.6553 (23) | 0.2167 (19) | 4.9 (7) |
| O(3) | 0.754 (4) | 0.9247 (22) | 0.1005 (18) | 4.5 (6) |
| O(4) | 0.002 (3) | 1.0919 (19) | 0.1733 (16) | 3.6 (5) |
| O(5) | 0.079 (4) | 0.8846 (22) | −0.0045 (18) | 4.6 (6) |
| O(6) | 0.464 (4) | 1.0962 (21) | 0.0514 (17) | 4.2 (6) |
| O(7) | 0.358 (3) | 0.6360 (20) | 0.2923 (16) | 3.7 (5) |
| O(8) | 0.036 (4) | 0.7365 (21) | 0.1219 (17) | 4.3 (6) |
| H(9) | 0.149 | 0.748 | 0.405 | 3.6 |
| H(10) | 0.285 | 0.909 | 0.415 | 3.4 |
| H(11) | 0.151 | 1.013 | 0.315 | 3.9 |
| H(12) | −0.089 | 0.928 | 0.244 | 3.6 |
| H(13) | −0.091 | 0.759 | 0.296 | 3.6 |
| H(17) | 0.617 | 1.034 | 0.337 | 3.7 |
| H(18) | 0.786 | 1.049 | 0.453 | 4.9 |
| H(19) | 0.877 | 0.913 | 0.520 | 5.5 |
| H(20) | 0.762 | 0.768 | 0.487 | 4.4 |
| H(21) | 0.587 | 0.752 | 0.370 | 3.7 |

$^a$ $B_{iso}$ is the mean of the principal axes of the thermal ellipsoid.

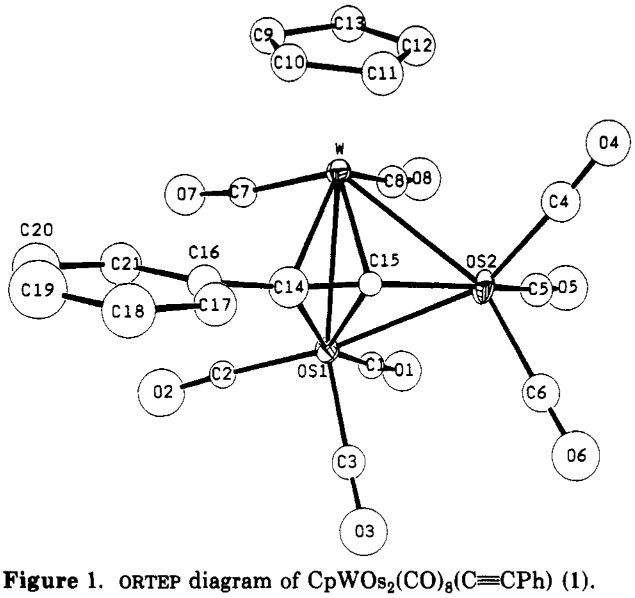

**Figure 1.** ORTEP diagram of $CpWOs_2(CO)_8(C{\equiv}CPh)$ (1).

(1)-C(15) = 2.16 (3) Å, and Os(2)-C(15) = 1.96 (3) Å and with its β-carbon linked to W and Os(1) atoms with distances Os(1)-C(14) = 2.17 (4) Å and W-C(14) = 2.36 (4) Å. The acetylide C-C bond distance (1.23 (5) Å) in this compound is only a little longer than the average C-C distance of acetylene molecules (1.20 Å).[24]

**Table III. Atomic Coordinates and Equivalent Isotropic Displacement Coefficients for $CpWRu_2(CO)_8(C{\equiv}CPh)$ (4)**

| | $x$ | $y$ | $z$ | $B_{iso}$,$^a$ Å$^2$ |
|---|---|---|---|---|
| W | 0.06565 (3) | 0.152711 (25) | 0.232915 (24) | 2.226 (14) |
| Ru(1) | 0.01359 (5) | 0.25009 (5) | 0.42250 (5) | 2.57 (3) |
| Ru(2) | −0.06312 (5) | 0.33911 (5) | 0.24900 (5) | 2.53 (3) |
| C(1) | 0.1463 (7) | 0.3217 (6) | 0.4574 (6) | 3.0 (4) |
| C(2) | 0.0384 (7) | 0.1407 (7) | 0.5210 (6) | 3.3 (4) |
| C(3) | −0.0590 (8) | 0.3353 (8) | 0.5028 (7) | 4.4 (5) |
| C(4) | −0.1360 (7) | 0.3451 (7) | 0.1146 (7) | 3.6 (4) |
| C(5) | 0.0559 (7) | 0.4236 (6) | 0.2284 (7) | 3.6 (4) |
| C(6) | −0.1425 (8) | 0.4459 (7) | 0.3009 (7) | 4.3 (5) |
| C(7) | 0.1303 (7) | 0.0634 (7) | 0.3440 (7) | 3.7 (4) |
| C(8) | 0.1938 (8) | 0.2410 (7) | 0.2635 (7) | 3.9 (4) |
| C(9) | 0.0571 (11) | 0.0034 (7) | 0.1469 (7) | 5.0 (6) |
| C(10) | −0.0335 (9) | 0.0565 (10) | 0.1074 (7) | 5.1 (6) |
| C(11) | 0.0016 (9) | 0.1431 (8) | 0.0610 (7) | 4.4 (5) |
| C(12) | 0.1128 (8) | 0.1409 (8) | 0.0721 (7) | 4.1 (5) |
| C(13) | 0.1507 (9) | 0.0560 (9) | 0.1232 (7) | 4.7 (5) |
| C(14) | −0.1503 (7) | 0.2249 (6) | 0.3243 (6) | 2.6 (4) |
| C(15) | −0.0687 (7) | 0.1789 (5) | 0.2912 (6) | 2.4 (3) |
| C(16) | −0.2617 (6) | 0.2087 (6) | 0.3451 (6) | 2.4 (3) |
| C(17) | −0.3468 (7) | 0.2556 (7) | 0.2886 (7) | 3.6 (4) |
| C(18) | −0.4510 (8) | 0.2338 (8) | 0.3003 (8) | 4.6 (5) |
| C(19) | −0.4724 (8) | 0.1642 (8) | 0.3706 (9) | 4.7 (5) |
| C(20) | −0.3890 (9) | 0.1175 (8) | 0.4289 (7) | 4.6 (5) |
| C(21) | −0.2823 (7) | 0.1390 (7) | 0.4179 (7) | 3.8 (4) |
| O(1) | 0.2222 (6) | 0.3666 (6) | 0.4774 (5) | 5.7 (4) |
| O(2) | 0.0583 (6) | 0.0838 (5) | 0.5830 (5) | 5.5 (4) |
| O(3) | −0.1027 (7) | 0.3884 (7) | 0.5503 (6) | 7.6 (5) |
| O(4) | −0.1778 (6) | 0.3511 (6) | 0.0335 (5) | 5.5 (4) |
| O(5) | 0.1245 (6) | 0.4739 (5) | 0.2174 (6) | 6.4 (4) |
| O(6) | −0.1908 (8) | 0.5078 (6) | 0.3305 (6) | 7.6 (5) |
| O(7) | 0.1733 (6) | 0.0066 (5) | 0.3995 (5) | 5.4 (4) |
| O(8) | 0.2736 (6) | 0.2861 (6) | 0.2734 (6) | 6.1 (4) |
| H(9) | 0.055 | −0.062 | 0.186 | 5.1 |
| H(10) | −0.113 | 0.038 | 0.111 | 5.4 |
| H(11) | −0.047 | 0.198 | 0.025 | 4.8 |
| H(12) | 0.160 | 0.196 | 0.046 | 4.6 |
| H(13) | 0.227 | 0.032 | 0.140 | 5.1 |
| H(17) | −0.331 | 0.310 | 0.237 | 4.4 |
| H(18) | −0.515 | 0.268 | 0.257 | 5.2 |
| H(19) | −0.550 | 0.149 | 0.381 | 4.9 |
| H(20) | −0.406 | 0.065 | 0.482 | 5.3 |
| H(21) | −0.221 | 0.104 | 0.464 | 4.5 |

$^a$ $B_{iso}$ is the mean of the principal axes of the thermal ellipsoid.

The most salient feature of the structure is the orientation of the acetylide moiety, which is σ-bonded to an Os atom and at the same time forms a transverse bridge across the second W-Os bond. Therefore, the structure of 1 is related to the $CpWFe_2(CO)_8(C{\equiv}CTol)$ by a 120° rotation of the acetylide ligand. The heterometallic acetylide cluster $CpNiFe_2(CO)_6(C{\equiv}C^tBu)$ also shows a similar asymmetric arrangement.[25]

**Description of the Solution Dynamics of the $WOs_2$ Complexes.** The acetylide ligand of these $WOs_2$ complexes is static on the time scale of $^{13}C$ NMR spectroscopy. The $^{13}C$ NMR spectrum of a $^{13}CO$-enriched sample of complex 1 exhibits two W-CO signals at δ 208.6 and 204.0, a sharp $Os(CO)_3$ signal at δ 179.7, and two very broad Os-CO signals at δ 178.8 and 173.4 at 295 K in toluene-$d_8$. When the temperature was increased to 350 K, the $Os(CO)_3$ signal at δ 179.7 remained unchanged but the broad Os-CO signals at δ 178.8 and 173.4 merged into a sharp signal at δ 176.5. This behavior is consistent with the presence of two, independent, localized 3-fold exchanges of the CO ligands of the $Os(CO)_3$ unit. One 3-fold rotation,

---

(24) March, J. *Advanced Organic Chemistry*, 3rd ed.; Wiley: New York, 1985; Chapter 1.

(25) Martinetti, A.; Sappa, E.; Tiripicchio, A.; Camellini, M. T. *J. Organomet. Chem.* **1980**, *197*, 335.

**Table IV. Atomic Coordinates and Equivalent Isotropic Displacement Coefficients for $CpMoRu_2(CO)_8(C\equiv CPh)$ (10)**

| | *x* | *y* | *z* | $B_{iso}$,[a] Å$^2$ |
|---|---|---|---|---|
| Ru(1) | 0.71869 (4) | 0.46159 (7) | 0.070708 (25) | 2.403 (22) |
| Ru(2) | 0.87172 (4) | 0.22655 (8) | 0.09524 (3) | 2.97 (3) |
| Mo | 0.73598 (5) | 0.34163 (8) | 0.19495 (3) | 2.62 (3) |
| C(1) | 0.5996 (6) | 0.6026 (10) | 0.0627 (4) | 3.8 (4) |
| C(2) | 0.7169 (6) | 0.4012 (9) | −0.0146 (3) | 3.3 (3) |
| C(3) | 0.8218 (6) | 0.6254 (10) | 0.0594 (4) | 4.2 (4) |
| C(4) | 0.8887 (6) | 0.1398 (9) | 0.0139 (4) | 3.6 (4) |
| C(5) | 0.9978 (6) | 0.3537 (12) | 0.0937 (4) | 5.3 (5) |
| C(6) | 0.9385 (6) | 0.0524 (11) | 0.1400 (4) | 4.7 (4) |
| C(7) | 0.8640 (6) | 0.4783 (10) | 0.1937 (3) | 3.9 (4) |
| C(8) | 0.6627 (6) | 0.5566 (10) | 0.1956 (3) | 4.0 (4) |
| C(9) | 0.7400 (12) | 0.0920 (12) | 0.2470 (4) | 7.1 (6) |
| C(10) | 0.8106 (7) | 0.1975 (14) | 0.2767 (4) | 5.4 (5) |
| C(11) | 0.7576 (9) | 0.3200 (12) | 0.3024 (4) | 5.4 (5) |
| C(12) | 0.6509 (9) | 0.2983 (16) | 0.2889 (5) | 7.5 (6) |
| C(13) | 0.6412 (9) | 0.1552 (17) | 0.2538 (4) | 7.4 (6) |
| C(14) | 0.7203 (5) | 0.2079 (8) | 0.1044 (3) | 2.4 (3) |
| C(15) | 0.6274 (5) | 0.2643 (8) | 0.1149 (3) | 2.2 (3) |
| C(16) | 0.5142 (5) | 0.2296 (8) | 0.1100 (3) | 2.4 (3) |
| C(17) | 0.4394 (5) | 0.3283 (9) | 0.1362 (3) | 3.8 (3) |
| C(18) | 0.3339 (5) | 0.2930 (10) | 0.1280 (4) | 4.0 (4) |
| C(19) | 0.3015 (6) | 0.1626 (10) | 0.0942 (4) | 4.1 (4) |
| C(20) | 0.3744 (6) | 0.0641 (10) | 0.0681 (4) | 4.9 (4) |
| C(21) | 0.4796 (6) | 0.0917 (9) | 0.0764 (3) | 3.8 (3) |
| O(1) | 0.5275 (5) | 0.6812 (8) | 0.0572 (3) | 6.6 (3) |
| O(2) | 0.7181 (4) | 0.3595 (7) | −0.06550 (23) | 5.0 (3) |
| O(3) | 0.8822 (5) | 0.7242 (8) | 0.0516 (3) | 7.0 (4) |
| O(4) | 0.8967 (4) | 0.0877 (7) | −0.0349 (3) | 5.5 (3) |
| O(5) | 1.0699 (5) | 0.4355 (9) | 0.0903 (3) | 8.8 (4) |
| O(6) | 0.9755 (5) | −0.0548 (8) | 0.1667 (3) | 7.7 (4) |
| O(7) | 0.9347 (4) | 0.5666 (8) | 0.2014 (3) | 6.2 (3) |
| O(8) | 0.6222 (5) | 0.6797 (7) | 0.2035 (3) | 6.1 (3) |
| H(9) | 0.756 | −0.012 | 0.225 | 6.0 |
| H(10) | 0.886 | 0.181 | 0.278 | 5.1 |
| H(11) | 0.787 | 0.413 | 0.327 | 5.5 |
| H(12) | 0.589 | 0.370 | 0.300 | 6.7 |
| H(13) | 0.577 | 0.104 | 0.238 | 6.0 |
| H(17) | 0.461 | 0.420 | 0.163 | 4.1 |
| H(18) | 0.282 | 0.363 | 0.147 | 4.4 |
| H(19) | 0.227 | 0.132 | 0.089 | 4.8 |
| H(20) | 0.352 | −0.026 | 0.041 | 5.2 |
| H(21) | 0.530 | 0.012 | 0.060 | 4.3 |

[a] $B_{iso}$ is the mean of the principal axes of the thermal ellipsoid.

**Table V. Relevant Bond Distances (Å) and Angles (deg) of $CpWOs_2(CO)_8(C\equiv CPh)$ (1)**

| | | | |
|---|---|---|---|
| (A) Bond Distances | | | |
| W–Os(1) | 2.830 (2) | W–Os(2) | 2.916 (2) |
| Os(1)–Os(2) | 2.814 (2) | W–C(15) | 2.20 (3) |
| Os(1)–C(15) | 2.16 (3) | Os(2)–C(15) | 1.96 (3) |
| Os(1)–C(14) | 2.17 (4) | W–C(14) | 2.36 (4) |
| C(14)–C(15) | 1.23 (5) | C(16)–C(14) | 1.47 (5) |
| W–CO (mean) | 1.97 (3) | Os–CO (mean) | 1.87 (3) |
| (B) Bond Angles | | | |
| Os(2)–C(15)–C(14) | 159 (3) | C(15)–C(14)–C(16) | 148 (4) |
| W–C–O (mean) | 172 (3) | Os–C–O (mean) | 176 (3) |

**Table VI. Relevant Bond Distances (Å) and Angles (deg) of $CpWRu_2(CO)_8(C\equiv CPh)$ (4)**

| | | | |
|---|---|---|---|
| (A) Bond Distances | | | |
| W–Ru(1) | 2.998 (1) | W–Ru(2) | 2.965 (1) |
| Ru(1)–Ru(2) | 2.661 (1) | W–C(15) | 1.976 (8) |
| Ru(1)–C(15) | 2.128 (8) | Ru(2)–C(15) | 2.195 (7) |
| Ru(1)–C(14) | 2.297 (8) | Ru(2)–C(14) | 2.188 (8) |
| C(14)–C(15) | 1.31 (1) | C(16)–C(14) | 1.47 (1) |
| W–CO (mean) | 1.979 (9) | Ru–CO (mean) | 1.910 (9) |
| (B) Bond Angles | | | |
| W–C(15)–C(14) | 162.5 (6) | C(15)–C(14)–C(16) | 142.5 (8) |
| W–C–O (mean) | 172.1 (8) | Ru–C–O (mean) | 177.6 (9) |

**Table VII. Relevant Bond Distances (Å) and Angles (deg) of $CpMoRu_2(CO)_8(C\equiv CPh)$ (10)**

| | | | |
|---|---|---|---|
| (A) Bond Distances | | | |
| Mo–Ru(1) | 2.828 (1) | Mo–Ru(2) | 2.927 (1) |
| Ru(1)–Ru(2) | 2.784 (1) | Mo–C(14) | 2.223 (6) |
| Ru(1)–C(14) | 2.198 (6) | Ru(2)–C(14) | 1.954 (6) |
| Ru(1)–C(15) | 2.214 (6) | Mo–C(15) | 2.265 (6) |
| C(14)–C(15) | 1.296 (9) | C(15)–C(16) | 1.475 (9) |
| Mo–CO (mean) | 1.988 (8) | Ru–CO (mean) | 1.902 (8) |
| (B) Bond Angles | | | |
| Ru(2)–C(14)–C(15) | 154.2 (5) | C(14)–C(15)–C(16) | 144.9 (6) |
| Mo–C–O (mean) | 171.0 (7) | Ru–C–O (mean) | 177.6 (7) |

**Table VIII. Numbering Scheme and the Relative Abundance of the Acetylide Derivatives of Type $LMM'_2(CO)_8(C\equiv CR)$**

| L | M | M′ | R | rel abundance of each isomer | | | |
|---|---|---|---|---|---|---|---|
| Cp | W | Os | Ph | **1a** | 100% | | |
| Cp* | W | Os | Ph | **2a** | 100% | | |
| Cp | W | Os | $^nBu$ | **3a** | 100% | | |
| Cp | W | Ru | Ph | **4a** | 45% | **4b** | 55% |
| Cp* | W | Ru | Ph | **5a** | 15% | **5b** | 85% |
| Cp | W | Ru | $C_6H_4F$ | **6a** | 45% | **6b** | 55% |
| Cp | W | Ru | $C_6H_4OMe$ | **7a** | 41% | **7b** | 59% |
| Cp | W | Ru | $^tBu$ | **8a** | 4% | **8b** | 96% |
| Cp | W | Ru | $^nPr$ | **9a** | 20% | **9b** | 80% |
| Cp | Mo | Ru | Ph | **10a** | 100% | | |
| Cp* | Mo | Ru | Ph | **11a** | 100% | | |
| Cp | Mo | Ru | $^tBu$ | **12a** | 95% | **12b** | 5% |
| Cp* | Mo | Ru | $^tBu$ | | | **13b** | 100% |
| Cp | Mo | Ru | $C_6H_4F$ | **14a** | 100% | | |

having a lower energy barrier, produces the sharp signals at δ 179.7 at room temperature; the second, having a relatively greater activation barrier, reaches the limit of fast exchange at higher temperature. In contrast, rotation of the $CpW(CO)_2$ unit cannot be observed because the two CO ligands on the tungsten atom are diastereotopic. The coalescences of the two W–CO signals and of the two $Os(CO)_3$ signals were not observed even at 370 K, suggesting that the racemization of 1 has not occurred at this temperature.

**Preparation and Characterization of the $WRu_2$ Complexes.** In order to investigate the preferred orientation of the acetylide ligand over the triangular face of the heterometallic complexes, we have carried out the syntheses of several $WRu_2$ derivatives. Complexes (**4**, L = Cp, R = Ph; **5**, L = Cp*, R = Ph; **6**, L = Cp, R = $C_6H_4F$; **7**, L = Cp, R = $C_6H_4OMe$; **8**, L = Cp, R = $^tBu$; **9**, L = Cp, R = $^nPr$) were obtained in good yield from the reaction between $Ru_3(CO)_{12}$ and the corresponding tungsten acetylide in a 2:3 molar ratio. For these $WRu_2$ derivatives, the $^1H$ NMR spectra and IR spectra in the region of CO absorption suggest the presence of two isomers in solution (Table VIII). The assignment of each isomer is further confirmed by their characteristic $^{13}C$ NMR data.

In order to prove that the isomerization is due to the acetylide rotation, we have carried out the structural determination on complex 4. Crystals suitable for X-ray experiments were obtained by recrystallization from $CH_2Cl_2$–hexane at room temperature. Its molecular structure is shown in Figure 2, and selected bond angles and distances are summarized in Table VI. The $WRu_2$ triangle is nearly isosceles with the bond distances W–Ru(1) = 2.998 (1) Å, W–Ru(2) = 2.965 (1) Å, and Ru(1)–Ru(2) = 2.661 (1) Å. The tungsten atom is associated with two slightly bent CO ligands (∠W–C–O(mean) = 172.1 (8)°) in addition to a Cp ligand, and each ruthenium atom is linked to three linear CO ligands (∠Ru–C–O(mean) = 177.6 (9)°). Most interesting, the acetylide moiety is now σ-bonded to the W atom and, quasi-symmetrically, π-bonded to the two Ru atoms. Therefore, we conclude that the $WRu_2$ derivatives in the solid state are isostructural

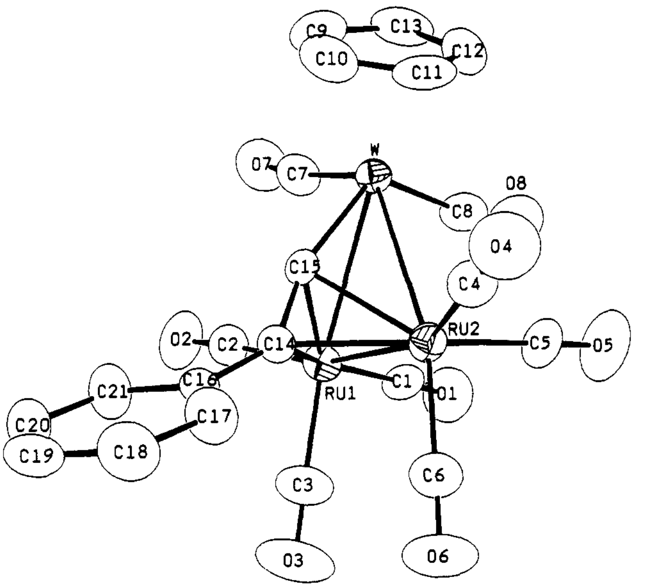

**Figure 2.** ORTEP diagram of $CpWRu_2(CO)_8(C{\equiv}CPh)$ (4).

Scheme I

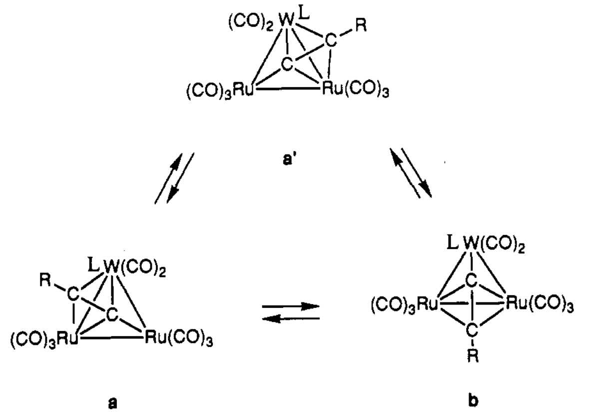

not with the $WOs_2$ derivatives but rather with the $WFe_2$ derivatives. The heterometallic acetylide clusters $CpWFe_2(CO)_8(C{\equiv}CTol)$[23] and $CoFe_2(CO)_9(C{\equiv}CSiMe_3)$[26] also exhibit a similar symmetric arrangement.

**Description of the $^{13}C$ NMR Spectra of the $WRu_2$ Complexes.** Both the $^1H$ NMR and IR $\nu(CO)$ spectra suggest the presence of two isomers in solution. The solution dynamics of these $WRu_2$ complexes are of particular interest. On the basis of the structural information established, we propose that the isomerization is caused by a 360° rotation of the acetylide ligand over the $WRu_2$ triangle (Scheme I). Before we proceed to discuss the rotation of the acetylide ligands, it is important to understand the assignment of each isomer and their relative abundance **a**/**b** in solution. The $^1H$ NMR and IR spectra failed to provide adequate information. Fortunately, $^{13}C$ NMR spectra in the region of CO resonances can reveal information on the overall molecular symmetry that allows us to assign the structure unambiguously.

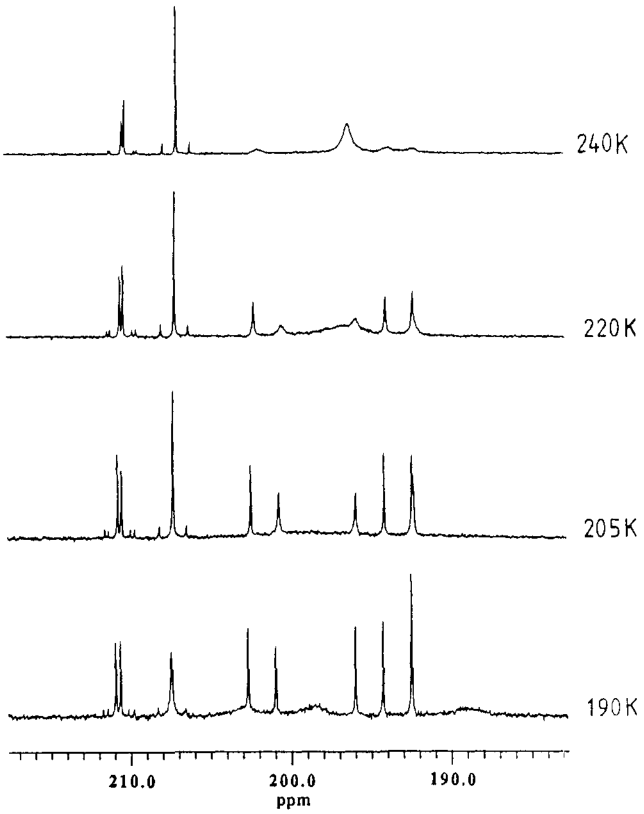

**Figure 3.** Variable-temperature $^{13}C$ NMR spectra ($CD_2Cl_2$) of 4, showing the region of CO resonances.

The $^{13}C$ NMR spectrum of 4 at 205 K exhibits three W-CO signals at $\delta$ 210.8, 210.5, and 207.3 in the ratio 1:1:2.4 (Figure 3). Therefore, the first two resonance lines are assigned to the "asymmetric" isomer (**4a**, the acetylide C-C bond bisects the W-Ru bond) and the third one to the "symmetric" isomer (**4b**, the acetylide C-C bond is orthogonal to the Ru-Ru bond). This assignment is reasonable because the CO ligands of the $CpW(CO)_2$ unit in the asymmetric isomer **4a** are diastereotopic, whereas in isomer **4b** the rotation of the $CpW(CO)_2$ fragment, having a relatively smaller activation barrier, would average the chemical environment of the CO ligands. Furthermore, five signals at $\delta$ 202.5, 200.8, 196.0, 194.2, and 192.4 with an intensity ratio of 1:1:1:1:2 are assigned to the Ru-CO resonances of **4a**; the signal at $\delta$ 192.4 is double the intensity of the other four signals and therefore corresponds to two coincident signals. The Ru-CO signals of **4b** were not observed at this temperature. However, when the temperature was decreased to 190 K, the W-CO signal of **4b** broadened and collapsed slightly, suggesting the slowing down of the $CpW(CO)_2$ rotation, and three very broad Ru-CO signals at $\delta$ 203.0, 198.5, and 189.0 appeared in the spectrum, consistent with the symmetric nature of **4b**. On the other hand, when the temperature was increased to 240 K, isomer **4b** showed a broad Ru-CO signal at $\delta$ 197.1, indicating the presence of a rapid 3-fold rotation of the $Ru(CO)_3$ unit. The other three weak Ru-CO signals at $\delta$ 202.9, 194.6, and 192.7 are assigned to isomer **4a**. Again, the localized $Ru(CO)_3$ rotation in **4a** is responsible for the observed NMR spectra.

Similar $^{13}C$ NMR spectra were also observed for other $WRu_2$ derivatives. The $^{13}C$ NMR spectrum of 8 at 294 K exhibits one W-CO signal at $\delta$ 208.4 and one Ru-CO signal at $\delta$ 198.0 in the ratio 1:3 assigned to isomer **8b**, in addition to two weak W-CO signals at $\delta$ 212.2 and 209.3 and one weak Ru-CO signal at $\delta$ 197.3 assigned to **8a** (Figure 4). Between 213 and 205 K the Ru-CO signals assigned to **8b** collapsed to the base line and six relatively weak Ru-CO signals of equal intensity at $\delta$ 204.6, 202.1, 198.0, 196.2, 194.4, and 193.6 emerged from the base line. We assign these six distinct Ru-CO signals to the asymmetric isomer **8a**.

When the temperature was decreased to 178 K, one broad W-CO signal at $\delta$ 208.9 and three broad Ru-CO

---

(26) Seyferth, D.; Hoke, J. B.; Rheingold, A. L.; Cowie, M.; Hunter, A. D. *Organometallics* **1988**, 7, 2163.

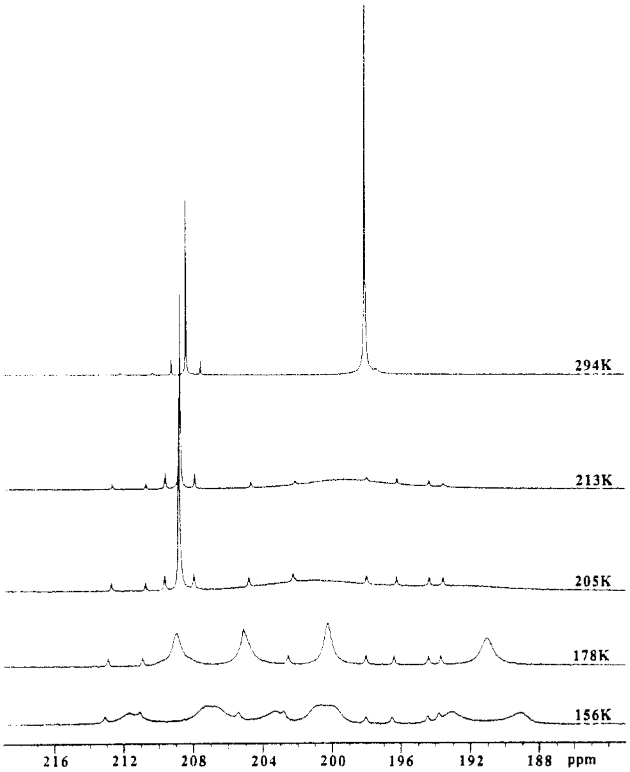

**Figure 4.** Variable-temperature $^{13}C$ NMR spectra ($CD_2Cl_2$) of 8, showing the region of CO resonances.

signals at δ 205.1, 200.2, and 191.0 of isomer **8b** were clearly observed. Further decreasing of the temperature to 156 K produced the splitting of these four signals, giving two W–CO signals at δ 211.6 and 206.7 and six Ru–CO signals at δ 207.2, 203.3, 200.8, 200.0, 193.1, and 189.1. We attribute the dynamic motion occurring between 178 and 156 K to the rotational motion of the $CpW(CO)_2$ unit. This rotational motion could be of a "pinwheel" type similar to the localized $Ru(CO)_3$ rotation[27] or a "swinging" motion with the bulky Cp ligand staying away from the acetylide. Both types of movements would average the environment of W–CO ligands and exhibit the observed fluxional behavior; unfortunately, our data are unable to distinguish them. From the coalescence temperature (178 K) of the W–CO signals, the activation free energy ($\Delta G^{\ddagger}$) for the rotation of the $CpW(CO)_2$ unit was estimated to be close to 3 kJ/mol.

Assignment of the $^{13}C$ NMR data of other $WRu_2$ derivatives is also based on the generalized experimental observation that the symmetric isomers **b** give one W–CO signal but the asymmetric isomers **a** give a pair of diastereotopic W–CO signals. After the major isomer in solution is established from the $^{13}C$ NMR data, the relative intensities of the corresponding Cp signals or the Cp* signals in the $^1H$ NMR spectrum reveal a more accurate ratio **a**/**b**. These data are listed in Table VIII.

**Rotation of the Acetylide Ligand on the $WRu_2$ Triangle.** The $^1H$ NMR spectrum of 4 in toluene-$d_8$ (Figure 5) shows two Cp signals at δ 4.78 and 4.58 in the ratio 1.2:1 at ambient temperature assigned to isomers **4b** and **4a**, respectively. When the system is warmed to 340 K, both Cp signals coalesce to a broad signal at δ 4.86, suggesting the beginning of the interconversion between **4a** and **4b**. The exchange observed is consistent with a 120° rotation (or the so-called edge hopping)[28] of the acetylide from a W–Ru edge to the Ru–Ru edge (**a** ⇔ **b** or **a**′ ⇔ **b**, Scheme I). From the coalescence temperature of 337 K for the Cp signals with chemical shift difference ($\Delta\nu$ = 80.0 Hz), an estimate for $\Delta G^{\ddagger}$ of 66 kJ/mol is obtained for the barrier of rotation. The kinetic parameters of other $WRu_2$ derivatives for this process, calculated from the data of the variable-temperature $^1H$ NMR studies, are summarized in Table IX.

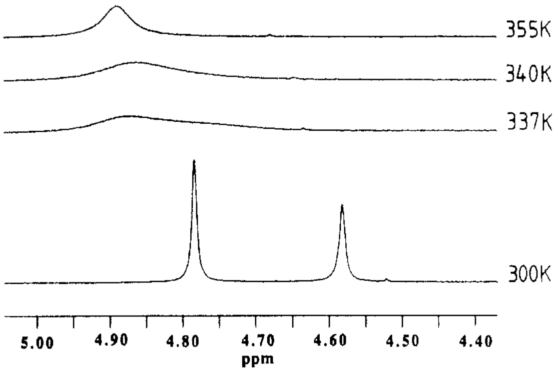

**Figure 5.** Variable-temperature $^1H$ NMR spectra (toluene-$d_8$) of 4 in the region of Cp resonances.

**Table IX. Free Energy ($\Delta G^{\ddagger}$) Data for the Acetylide Isomerization of $WRu_2$ Derivatives and Racemerization of $MoRu_2$ Derivatives**

| complex | L | R | $T_c$, K | $\Delta\nu$, Hz | $\Delta G^{\ddagger}$ kJ/mol |
|---|---|---|---|---|---|
| | | $WRu_2$ Derivatives | | | |
| 4 | Cp | ph | 337 | 80.0[a] | 68 |
| 6 | Cp | $C_6H_4F$ | 334 | 89.0[a] | 67 |
| 7 | Cp | $C_6H_4OMe$ | 300 | 72.9[a] | 61 |
| 9 | Cp | $^nPr$ | 353 | 75.7[a] | 72 |
| | | $MoRu_2$ Derivatives | | | |
| 10 | Cp | Ph | 338 | 163.0[b] | 67 |
| 11 | Cp* | Ph | 303 | 46.4[b] | 63 |

[a] The chemical shift difference between the Cp signals. [b] The chemical shift difference between the diastereotopic W–CO signals.

**Chart I**

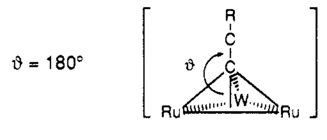

However, the second rotational process, racemization of **4a** (**a** ⇔ **a**′), consisting of a 120° rotation of the acetylide over the tungsten atom, cannot be examined by $^1H$ NMR studies. On the other hand, the appropriate evidence is deduced from the variable-temperature $^{13}C$ NMR data. The $^{13}C$ NMR spectrum of 4 in toluene-$d_8$ at 310 K (Figure S1 of the supplementary material) exhibits two W–CO signals at δ 212.0 and 211.5 for isomer **4a** and one W–CO signal at δ 208.5 for isomer **4b**. These three signals merge to the base line simultaneously on warming to 355 K and coalesce to a single line at δ 209.5 on further warming to 373 K, indicating that both the racemization (**a** ⇔ **a**′) and isomerization (**a** ⇔ **b**) occur at the same or about the same rate.[29] These observations indicate that the racemization may either (i) involve a 240° rotation of the tilted acetylide

---

[27] Rosenberg, E.; Thorsen-Thorsen, B.; Milone, L.; Aime, S. *Inorg. Chem.* **1985**, *24*, 231.

[28] Rosenberg, E.; Wang, J.; Gellert, R. W. *Organometallics* **1988**, *7*, 1093.

[29] The calculated chemical shift of the averaged W–CO signals (based on the chemical shifts at 310 K) for the exchange of the symmetric and the unsymmetric isomers is at δ 210.0. We believe that the small difference (0.5 ppm) is caused by the temperature dependence of the chemical shifts.

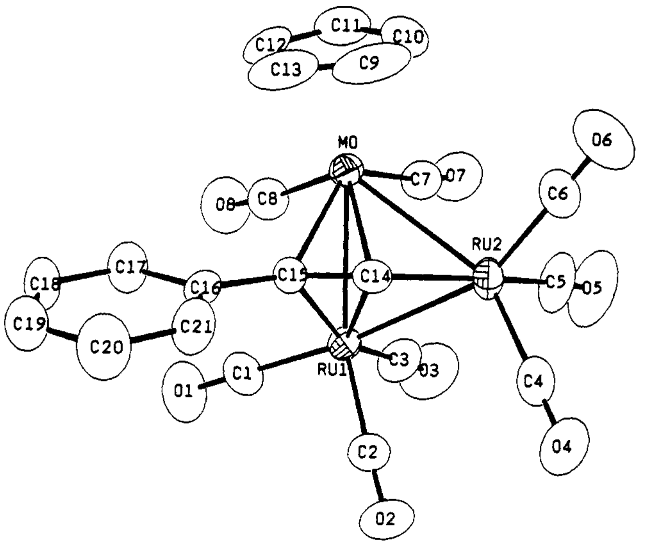

**Figure 6.** ORTEP diagram of $CpMoRu_2(CO)_8(C\equiv CPh)$ (**10**).

($\theta < 180°$) over both ruthenium atoms (**a** ⇔ **b** ⇔ **a′**) or (ii) involve a common transition state in which the acetylide C–C bond is perpendicular to the $WRu_2$ triangle (Chart I). The third possibility involving a direct 120° rotation of the tilted acetylide ($\theta < 180°$) over the tungsten atom (**a** ⇔ **a′**) is presumably a process with a slightly greater barrier because of the repulsion imposed by the bulky Cp ligand. Finally, although we are unable to eliminate the first and third possibilities involving the titled acetylide moiety, the second pathway involving the vertical acetylide moiety is preferred. The participation of a similar intermediate containing a vertical $C_2$ vinylidene moiety has been claimed to account for the isomerization of the ethoxyvinylidene ligands of the osmium cluster $H_2Os_3(CO)_9(C{=}CHOEt)$.[30]

**Preparation and Characterization of the MoRu$_2$ Complexes.** The related $MoRu_2$ derivatives (**10**, L = Cp, R = Ph; **11**, L = Cp*, R = Ph; **12**, L = Cp, R = $^tBu$; **13**, L = Cp*, R = $^tBu$; **14**, L = Cp, R = $C_6H_4F$) were synthesized from reactions between $Ru_3(CO)_{12}$ and the respective molybdenum acetylide under similar conditions. The X-ray structural determination on phenyl derivative **10** suggests that it has a structure similar to those of complex **1** and complex **12**,[28] both possessing the asymmetric arrangement (Figure 6). Consistent with the solid-state structure, its $^{13}C$ NMR spectrum at 215 K exhibits two Mo–CO signals at $\delta$ 226.4 and 225.3 and six Ru–CO signals at $\delta$ 202.6, 202.0, 196.6, 196.2, 194.3, and 193.7 (Figure S2). When the sample is warmed to 275 K, the signals at $\delta$ 202.6, 194.3, and 193.7 and at $\delta$ 202.2, 196.6, and 196.2 each coalesce to a singlet at $\delta$ 196.4 and a broad signal at $\delta$ 197.8, indicating the onset of the localized $Ru(CO)_3$ rotation. A similar structure was proposed for the respective Cp* derivative **11**; further support comes from the $^{13}C$ NMR spectrum at 244 K, which shows two Mo–CO singlets at $\delta$ 230.0 and 229.5 in the intensity ratio 1:1 and four Ru–CO signals at $\delta$ 201.4, 197.6, 193.7, and 192.8 in the ratio 1:3:1:1.

Although the assignment of complexes **10** and **11** in solution is straightforward, the assignment of the *tert*-butyl derivatives **12** and **13** is quite different. First, the IR spectrum of **12** in the region of CO absorptions indicates the existence of two isomers. The identity of each isomer is then confirmed by the $^{13}C$ NMR studies at 205 K, which show the expected eight-line pattern (two Mo–CO and six Ru–CO signals) at $\delta$ 225.9, 225.5, 204.0, 202.4, 197.4, 196.4, 194.8, and 194.3 assigned to isomer **12a** and the two-line pattern of isomer **12b** (one Mo–CO and Ru–CO signal) at $\delta$ 223.0 and 200.1 in the ratio 1:3. From the intensity ratio of $^{13}C$ NMR integration, the abundance **12a**:**12b** is calculated to be 19:1. This assignment is in contrast with that of the recently published report on **12**,[28] and the incorrect deduction was probably made because of the low concentration of **12b** in solution. Furthermore, the $^{13}C$ NMR spectrum of **13a** at 200 K exhibits one sharp Mo–CO signal at $\delta$ 227.0 and three broad Ru–CO signals at $\delta$ 207.0, 200.6, and 191.9 in the ratio 1:1:1:1, consistent with the adoption of a symmetric arrangement.

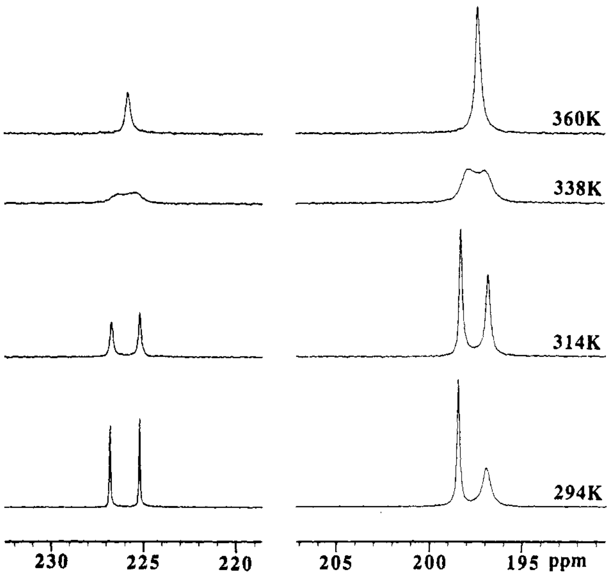

**Figure 7.** Variable-temperature $^{13}C$ NMR spectra (toluene-$d_8$) of **10** in the region of CO resonances.

**Scheme II**

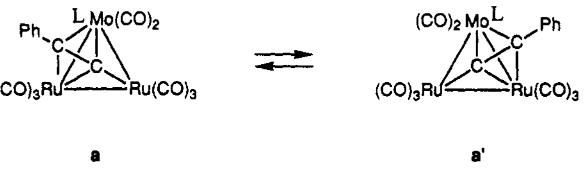

**Description of the Solution Dynamics of the MoRu$_2$ Complexes.** The acetylide ligand of the $MoRu_2$ complexes **10** and **11** is associated with one of the Mo–Ru bonds; therefore, its fluxional motion (Scheme II) can be examined by $^{13}C$ NMR studies. The $^{13}C$ NMR spectrum of **10** at 294 K (Figure 7) exhibits two Mo–CO signals at $\delta$ 226.8 and 225.2, a sharp $Ru(CO)_3$ signal at $\delta$ 198.4, and a broad $Ru(CO)_3$ signal at $\delta$ 196.9. When the temperature is increased gradually, the sharp Mo–CO signals start to broaden and the broad $Ru(CO)_3$ signals start to sharpen. However, both the Mo–CO and the $Ru(CO)_3$ signals collapse in a pairwise manner at 338 K, indicating that the molecule begins to acquire a time-averaged mirror plane. This observation cannot be explained according to the concept of intermetallic Ru–CO scrambling proposed for the $Ru_3(CO)_9(C\equiv C^tBu)^-$ anion.[31] Thus, we propose that a further fluxional process, i.e. migration of the acetylide

---

[30] Boyar, E.; Deeming, A. J.; Felix, M. S. B.; Kabir, S. E.; Adatia, T.; Bhusate, R.; McPartlin, M.; Powell, H. R. *J. Chem. Soc., Dalton Trans.* **1989**, 5.

[31] Barner-Thorsen, C.; Harcastle, K. I.; Rosenberg, E.; Siegel, J.; Manotti Landfredi, A. M.; Tiripicchio, A.; Tiripicchio Cammellini, M. *Inorg. Chem.* **1981**, *20*, 4306.

ligand from one Mo–Ru edge to the second, is evident.[28]

Furthermore, the coalescence of the diastereotopic M–CO signals of the Cp* derivative **11** takes place at 303 K (Figure S3, supplementary material). At 345 K, the $^{13}C$ spectrum exhibits a very sharp Mo–CO signal and a less sharp Ru–CO signal, indicating that the intermetallic CO scrambling between the Mo and Ru atoms has not occurred. The kinetic barriers for the acetylide migration are summarized in Table IX.

**Factors That Affect the Site Selectivity and Barrier of the Acetylide Rotation.** The transition-metal atoms, the accessory ligand, and even the substituent on the acetylide ligand have considerable impact on both the location of the acetylide and the barrier of its fluxional behavior. In general, the acetylide C–C vector tends to interact more strongly with the M–M bond in the order

$$\text{W–Os} > \text{Os–Os} \qquad \text{Mo–Ru} \geq \text{Ru–Ru} \geq \text{W–Ru}$$

Furthermore, the barrier of the acetylide migration of the $WOs_2$ derivatives is clearly larger than those of the $WRu_2$ and $MoRu_2$ derivatives.

The electron-releasing and bulky substituents on the acetylide ligand and the more electron-releasing and bulky Cp* ligands on tungsten or molybdenum prefer the structure of symmetric isomer **b**. The dependence on the nature of the substituent R is indicated from the comparison of the **a**:**b** ratio of the pairs between **5** and **7**, **5** and **8**, **8** and **9**, **10** and **12**, and **11** and **13**, whereas the **a**:**b** ratio of the pairs between **4** and **5** and **12** and **13** accounts for the influence of the Cp* ligand (Table VIII). The origin of the electronic effect is uncertain at present. However, the steric effect is clearly due to the repulsion between the ligand L and the substituent R; the steric crowding between L and R of the symmetric isomer **b** is evidently smaller than that of the asymmetric isomer **a**.

The activation barrier of the acetylide migration shows values in the narrow range 61–72 kJ/mol (Table IX). From the variable-temperature NMR studies we conclude that the barriers for the rotation of the acetylide are much greater than those for the 3-fold localized rotation of the $CpW(CO)_2$, $CpMo(CO)_2$, and $Ru(CO)_3$ moieties in this system. The variation in these values also indicates that the barriers decreased when there is a better electron-releasing substituent R on acetylide or a better donor ligand Cp* on the transition-metal atom. This finding is in good agreement with our proposal that, in the transition state of the acetylide migration, the acetylide is perpendicular to the metal triangle; accordingly, the bonding interaction between the $\beta$-carbon and the metal atoms is weakened substantially. An electron-releasing substituent on the $\beta$-carbon and the Cp* ligand on the basal metal atom would definitely stabilize the transition state and decrease the barrier. This interpretation is valid even in the case in which the acetylide moiety adopts a tilted arrangement in the transition state ($\theta < 180°$).

**Acknowledgment.** We are grateful to the National Science Council of the Republic of China for financial support (Grant No. NSC79-2008-M007-52).

**Supplementary Material Available:** Three variable-temperature $^{13}C$ NMR spectra (Figures S1–S3) and tables of nonessential bond distances and angles and anisotropic thermal parameters for **1**, **4**, and **10** (12 pages); listings of the observed and calculated structural factors for **1**, **4**, and **10** (37 pages). Ordering information is given on any current masthead page.

---

# Bimetallic Macrocyclic Zirconocene Dialkoxides: Synthesis, Structure, Bonding, and Molecular Modeling Considerations

Douglas W. Stephan

*Department of Chemistry and Biochemistry, University of Windsor, Windsor, Ontario, Canada N9B 3P4*

*Received March 1, 1990*

The reactions of $Cp_2ZrMe_2$ with the diols 2,2-dimethylpropane-1,3-diol and 1,3-benzenedimethanol proceed with evolution of methane, affording the macrocyclic zirconocene dialkoxides $Cp_2Zr(\mu\text{-}OCH_2C(CH_3)_2CH_2O)_2ZrCp_2$ (**1**) and $Cp_2Zr(\mu\text{-}OCH_2C_6H_4CH_2O)_2ZrCp_2$ (**2**), respectively. Complex **1** crystallizes in the tetragonal space group $P4_2mnm$ with $a = 8.585$ (2) Å, $c = 20.200$ (2) Å, $Z = 2$, and $V = 1448.7$ (5) Å$^3$. Molecule **2** crystallizes in the trigonal space group $R\bar{3}$ with $a = 18.976$ (4) Å, $Z = 3$, and $V = 2485.6$ (8) Å$^3$. In the case of **1**, a disorder in the structural data is consistent with two possible conformations of the 12-membered dimetalated ring. Molecular mechanics calculations in which the geometry at Zr is fixed were performed for the two possible conformers. The pseudocrown conformation is predicted to be thermodynamically more stable than the pseudochair form. In contrast, complex **2** adopts a pseudochair conformation. In addition, the disposition of the alkyl substituents on the oxygen atoms is endo for **1** and exo for **2**. These structural differences between **1** and **2** are considered and discussed. The nature of the Zr–O bonding in these complexes is discussed in terms of the extended Hückel molecular orbital picture. The structural and theoretical data support the notion of significant $\pi$-bonding between Zr and oxygen.

## Introduction

Early-metal oxides such as titania and zirconia are often employed as support materials for heterogeneous catalysts.[1] The support may act simply as a dispersent for the late-metal centers or may play an active role in the catalytic cycle. The latter instance gives rise to the phenomenon known as strong metal–support interactions (SMSI).[1] Cooperative activation of substrate molecules by a Lewis acidic early-metal center and a late-metal center has been proposed to account for this effect. Recent studies have investigated homogeneous systems in which early and late metals are linked in close proximity by bridging ligands.[2] Such heterobimetallics are of interest

---

[1] (a) *Metal-Support Interactions in Catalysis, Sintering, and Redispersion*; Stevenson, S. A., Dumesic, J. A., Baker, R. T. K., Ruckenstein, E., Eds.; Van Nostrand-Reinhold: New York, 1987. (b) *Strong Metal-Support Interactions*; Baker, R. T. K., Tauster, S. J., Dumesic, J. A., Eds.; American Chemical Society: Washington, DC, 1986.

0276-7333/90/2309-2718$02.50/0